AD_____

Award Number: DAMD17-02-1-0097

TITLE: Prostate Carcinoma Detection Using Combined Ultrasound, Elasticity, and Tissue Strain-Hardening Imaging

PRINCIPAL INVESTIGATOR: Stanislav Y. Emelianov, Ph.D.

CONTRACTING ORGANIZATION: The University of Michigan
Ann Arbor, Michigan 48109-1274

REPORT DATE: January 2003

TYPE OF REPORT: Annual

PREPARED FOR: U.S. Army Medical Research and Materiel Command
Fort Detrick, Maryland 21702-5012

REPORT DOCUMENTATION PAGE

Form Approved
OMB No. 074-0188

1. AGENCY USE ONLY (Leave blank)	2. REPORT DATE	3. REPORT TYPE AND DATES COVERED
	January 2003	Annual (31 Dec 2001 - 30 Dec 2002)

4. TITLE AND SUBTITLE
Prostate Carcinoma Detection Using Combined Ultrasound, Elasticity, and Tissue Strain-Hardening Imaging

5. FUNDING NUMBERS
DAMD17-02-1-0097

6. AUTHOR(S)
Stanislav Y. Emelianov, Ph.D.

7. PERFORMING ORGANIZATION NAME(S) AND ADDRESS(ES)
The University of Michigan
Ann Arbor, Michigan 48109-1274

E-Mail: emelian@mail.utexas.edu

8. PERFORMING ORGANIZATION REPORT NUMBER

9. SPONSORING / MONITORING AGENCY NAME(S) AND ADDRESS(ES)
U.S. Army Medical Research and Materiel Command
Fort Detrick, Maryland 21702-5012

10. SPONSORING / MONITORING AGENCY REPORT NUMBER

11. SUPPLEMENTARY NOTES

12a. DISTRIBUTION / AVAILABILITY STATEMENT
Approved for Public Release; Distribution Unlimited

12b. DISTRIBUTION CODE

13. ABSTRACT (Maximum 200 Words)

The underlying hypothesis of our study is that remote, non-invasive measurements of elasticity in prostate glands are possible and provide unique examiner-independent information which could increase the detection and/or characterization of potentially malignant masses in the prostate not accessible to manual palpation. The purpose of this study is to develop ultrasound technology to produce high-resolution displacement and strain data throughout the prostate for remote evaluation of the strain dependent elastic (Young's or shear) modulus. To this end, the main objective of the research program is to test the hypothesis that quantitative elasticity images of the prostate can be obtained with real-time ultrasound. To achieve this objective, we have developed speckle tracking algorithms and methods for strain and elasticity imaging of prostate. These studies include adaptive displacement and strain imaging, incompressibility processing and strain-hardening imaging. Next, we will test the developed methods using tissue-mimicking and tissue-containing phantoms, and well-defined clinical studies. At the conclusion of the study, a prototype of clinical prostate ultrasound elasticity imager will be designed. The overall program is designed to demonstrate that combined ultrasound, elasticity and strain-hardening imaging permits surrogate, remote palpation of the prostate gland.

14. SUBJECT TERMS
Prostate Carcinoma, Medical Imaging, Ultrasound, Elasticity

15. NUMBER OF PAGES
12

16. PRICE CODE

17. SECURITY CLASSIFICATION OF REPORT	18. SECURITY CLASSIFICATION OF THIS PAGE	19. SECURITY CLASSIFICATION OF ABSTRACT	20. LIMITATION OF ABSTRACT
Unclassified	Unclassified	Unclassified	Unlimited

Table of Contents

INTRODUCTION:

Great progress has been made in the last decade in prostate ultrasound imaging. It is the fundamental premise of this proposal, however, that current prostate imaging devices can be dramatically improved to provide more diagnostic information. The underlying hypothesis of our study is that remote, non-invasive measurements of elasticity in prostate glands are possible and provide unique examiner-independent information which could increase the detection and/or characterization of potentially malignant masses in the prostate not accessible to manual palpation. The purpose of this study is to develop ultrasound technology to produce high-resolution displacement and strain data throughout the prostate for remote evaluation of the strain dependent elastic (Young's or shear) modulus. To this end, the main objective of the research program is to test the hypothesis that quantitative elasticity images of the prostate, that is images of the strain dependent elastic (Young's) modulus, can be obtained with real-time ultrasound. To achieve this objective, we will (1) develop algorithms for ultrasound speckle tracking, strain imaging and tissue strain-hardening mapping, (2) test developed techniques using both tissue-mimicking phantoms and the prostate autopsies, and (3) validate combined ultrasound, elasticity and strain-hardening imaging on a group of patients undergoing ultrasound-guided biopsies and radical prostatectomies, and design a prototype of a clinical elasticity imager. The overall program is designed to demonstrate that combined ultrasound, elasticity and strain-hardening imaging permits surrogate, remote palpation of the prostate gland.

BODY:

Cancer of the prostate is a significant source of morbidity and mortality among men, accounting for 21% of cancers and 11% of cancer deaths in 1989. It is second in prevalence only to lung cancer [Silverberg and Lubera 1989]. These numbers have not significantly changed in the recent decade [ACS 2002]. There is, therefore, a desperate need for a reliable, non-invasive technique for early detection of prostatic cancer.

Changes in soft tissue elasticity are usually related to some abnormal, pathological process. The success of the digital rectal examination (DRE) as a diagnostic tool for detecting prostate carcinoma is evidence of this. Even today, DRE is widely used by primary care physicians and medical specialists, in conjunction with transrectal ultrasound (TRUS) and laboratory measurements such as serum prostate-specific antigen (PSA) concentration. The efficacy of DRE, however, is limited to relatively large (on the order of 10 mm) abnormalities located in the posterior portion of the prostate gland. Nevertheless, differences in Young's or shear modulus (i.e., the quantitative measure related to the information obtained by DRE) between tissue types can be many orders of magnitude [Sarvazyan 1975; Sarvazyan et al. 1993 and 1995; Parker et al. 1990]. Unfortunately, no conventional imaging modality, including ultrasound, nuclear magnetic resonance (MRI) or computed tomography (CT), can directly provide information about tissue elasticity. However, imaging modalities such as MRI and ultrasound can be used to measure internal motion induced by external deformations (i.e., deformations applied at the rectal wall), from which the elastic properties of the prostate can be **reconstructed** [O'Donnell et al. 1993 and 1994; Skovoroda et al. 1994, 1995 and 1998; Emelianov et al.

1995a and 1995b; Chenevert et al. 1997a and 1997b]. Elasticity imaging, therefore, consists of three main components: 1) evaluation of externally induced internal tissue motion using imaging devices, 2) measurement of strain tensor components and, finally, 3) reconstruction of the spatial distribution of the elastic modulus using displacement and strain images. Although other imaging modalities monitor internal tissue motion, elasticity imaging represents a **fundamentally new diagnostic modality** providing information not accessible by conventional imaging [Ophir et al. 1996, Gao et al. 1996].

In principle, any imaging modality and various deformation procedures can be used for elasticity measurement. Work over the last several years has shown that ultrasound and MRI are the preferred imaging modalities since both can exploit signal phase to sensitively track internal tissue motion [Ophir et al. 1996, Gao et al. 1996]. Similarly, researchers have explored both static and dynamic external deformations to induce internal tissue motion. For the specific application of prostate cancer detection with elasticity imaging, ultrasound measurement of static deformations appears optimal. Since the prostate is typically located near the rectal wall surface, mechanical and ultrasound access are not obstructed by solid structures such as bone and undesired layers of fat or muscle tissue. This proximity of the prostate to the rectal wall insures that high frequency, and hence high spatial resolution, sonography, and thus elasticity imaging, is possible. Additionally, internal deformations can be easily created within the prostate using fairly simple deformation devices. During a short (typically of only a few seconds duration), continuous deformation producing only minimal patient discomfort, real-time ultrasound data can be captured over a wide range of internal strains permitting adaptive (i.e., strain-hardening) elasticity imaging. Because of this, our combined transrectal ultrasound, elasticity and **strain-hardening** imaging approach is new and unique compared to other elasticity imaging techniques.

An ambitious research plan has been developed to address important engineering and clinical aspects of AMI development. A very competitive group of researchers with extensive experience in elasticity imaging (Biomedical Engineering Department, University of Michigan, Ann Arbor, MI) and clinical radiology and pathology (University of Michigan Medical School, Ann Arbor, MI) with emphasis on prostate cancer diagnosis was formed for this project. The overall program was designed to critically test the hypothesis that quantitative elasticity images of the prostate, that is images of the strain dependent elastic (Young's) modulus, can be obtained with real-time ultrasound, thus providing a valuable clinical tool for both diagnosis, monitoring and therapy of prostate pathology. Specifically, we will first develop speckle tracking algorithms and methods for strain and elasticity imaging of prostate. These studies will include adaptive displacement and strain imaging, incompressibility processing and tissue strain-hardening imaging. Second, we will test the developed methods using tissue-mimicking and tissue-containing phantoms, and develop a 3-D model of prostate elasticity. We will further test the ultrasound elasticity imaging using well-defined clinical studies. Finally, all technical issues related to prostate ultrasound elasticity imaging including ultrasound probe and scan geometry, motion artifacts, optimization of strain measurements, and specific elasticity reconstruction algorithms will be addressed. At the conclusion of the study, a prototype of clinical prostate ultrasound elasticity imager will be designed. In the remainder of this section we present detailed results from each of the proposed areas.

Phantom and Deformation System Development

Based on the literature data (see example in Fig. 1), the material for adequate manufacturing of mechanical models of prostate should cover the range of Young's modulus from 1 to 100 kPa. In addition, a compatible material with Young's modulus on the order of 1MPa is needed to simulate the surrounding internal tissue including rectum wall. We have tested various polymer materials to reliably produce tissue-mimicking phantoms of a wide variety of sizes and internal complexities within these modulus ranges. Within the scope of this project, we constructed several phantoms to test the ability of the AMI to detect internal elasticity variations.

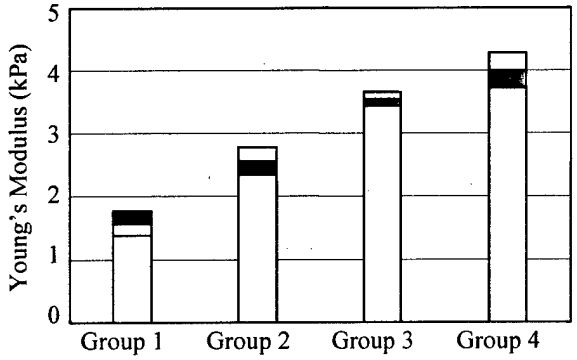

Group 1: Nodular hyperplasia with superimposed prostatitis
Group 2: Nodular hyperplasia with microcystic areas
Group 3: Fibromascular stroma between tubuloalveloar glands
Group 4: Stromal nodules in prostatic nodular hyperplasia

Figure 1: Summary of Young's elastic modulus measurements performed in 75 prostate tissue specimens from 28 men who underwent radical prostatectomy.

In the example below (Fig. 2), an *ex-vivo* human prostate was studied. Briefly, elasticity imaging experiments were performed on a normal prostate obtained at autopsy, embedded in an otherwise homogeneous gel-based phantom. This gel-based phantom was designed to mimic both the elastic and ultrasound properties of the prostate and surrounding soft tissue. At this stage, the phantom was primarily designed to address the initial critical issues determining whether elasticity imaging is capable of prostate cancer detection. Figures 2a and 2b are the conventional B-scans of the phantom with embedded prostate showing the geometry and location of the prostate within the phantom before and after deformation.

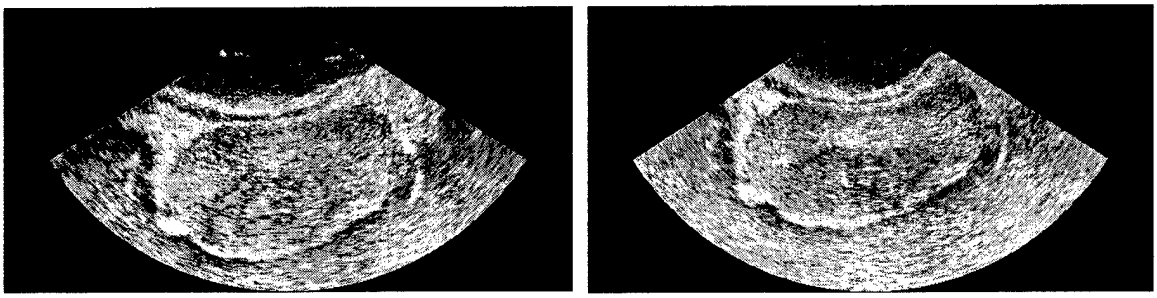

Figure 2: Conventional B-Scan images of the phantom with embedded prostate showing the geometry and location of the prostate within the phantom before and after deformation.

The *ex-vivo* phantom study was performed using a Siemens "Elegra" clinical ultrasound scanner equipped with an 6.5EC10 curved intracavitary array transducer operating in the 5 to 8 MHz frequency range. The experimental setup included the ultrasound intracavitary probe adapted for elasticity studies of the prostate. This probe was positioned in contact with modeled rectum wall (top of the images in Fig. 2) to

deform the wall and adjacent tissue including the prostate gland, where deformations were continuously imaged with ultrasound, and captured for off-line elasticity processing. Deformations were produced directly with the ultrasound probe. As the probe is gently pushed against the rectal wall (similar to palpation or DRE examination), controlled deformations are applied resulting in controlled deformation of the prostate and surrounding tissue.

Surface deformation was performed over 6 second interval while more than hundred phase-sensitive ultrasound frames were captured continuously and stored for off-line processing. Once baseline data were captured, one ml of 10 percent glutaraldehyde solution was very slowly injected into one site of the prostate creating a stiffer "hard" lesion. The injection was guided by real-time ultrasound imaging. After injection, deformation measurements were repeated 3.5 hours later to detect elasticity changes. Note that precisely the same cross-section of the prostate was imaged before, during, and after injection allowing quantitative monitoring of the gland. Finally, at the conclusion of the experiment, the phantom was cut along the imaging plane, and prostate tissue and surrounding gelatin were manually palpated to qualitatively assess the elasticity distribution before and after injection.

Data Acquisition and Initial Data processing

During deformation, more than a hundred of consecutive frames of the digital radio frequency (RF) signal output by the beamformer of a Siemens "Elegra" clinical ultrasound scanner were nondestructively captured in real-time. Initially, these data were rapidly processed to evaluate the quality of captured data. In particular, we have developed an algorithm to convert the captured signal and display B-scan cineloop in both unconverted (polar) and scan converted (rectangular) system of coordinates. The review of B-scan cineloop was performed to analyze the quality of the data. If the quality of captured data was acceptable, the data was stored for subsequent and complete off-line displacement/strain and elasticity processing.

Displacement and Strain Imaging

Once the deformation dataset was captured and quality of the captured data was confirmed, off-line processing was performed. The first step in the off-line processing is to estimate the motion between two (not necessarily adjacent) frames. The frame-to-frame motion was estimated using a two-dimensional correlation-based phase-sensitive speckle tracking technique. This particular technique combines the ability of correlation-based algorithms to track relatively large internal displacements with the precision of phase sensitive methods. First, frame-to-frame lateral and axial displacements were estimated from the position of the maximum correlation coefficient, where a correlation kernel approximately equaling the speckle spot is used for optimal strain estimation. The axial displacement estimate was then further refined by determining the zero crossing position of the phase of the analytic signal correlation. Frame-to-frame displacement error was also reduced using a weighted correlation sum and by filtering spatially adjacent correlation functions prior to displacement estimation. Furthermore, errors due to speckle decorrelation were reduced by accumulating incremental frame-to-frame displacements to produce total displacement and strain images with large average strains. It should be noted here that all images were accumulated to the original position representing the object before deformation. The normal axial strains were computed from accumulated axial displacements using a simple 1-D difference filter along the axial direction for correlation windows. The results of this experiment are given in Figures 3-7.

Figures 3a and 3b are the conventional B-scans of the phantom with embedded prostate showing the geometry and location of the prostate within the phantom before and after the injection of glutaraldehyde. These and all other images in Figure 1 are displayed over the same 120-mm (lateral) by 60-mm (axial) area. There are insignificant changes in the B-scan image (Fig. 3b), and these changes cannot be *a priori* related to glutaraldehyde injection confirming that ultrasound imaging alone is not sensitive to changes in mechanical properties of tissue.

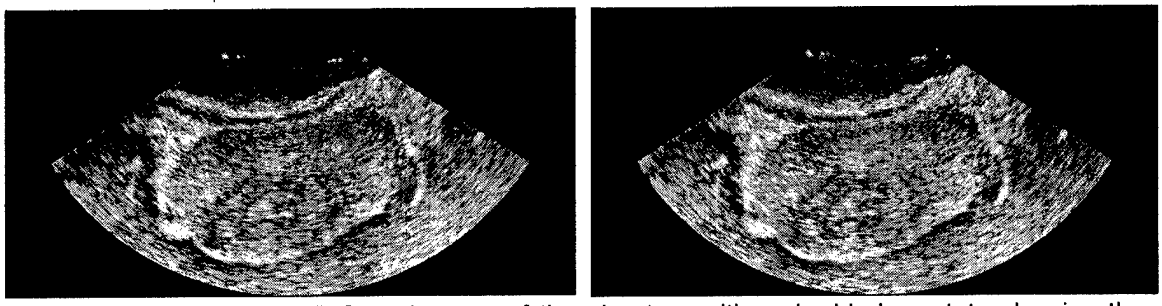

Figure 3: Conventional B-Scan images of the phantom with embedded prostate showing the geometry and location of the prostate within the phantom before and after the injection of glutaraldehyde. Note that there are no significant changes in B-scan images indicating that ultrasound imaging alone is not sensitive to changes in mechanical properties of tissue.

Figure 4 is a map of a normalized correlation coefficient displayed using a quantitative gray scale over 0.95-1.0 dynamic range. This image can be used to assess the quality of speckle tracking, i.e., how well the internal motion is measured. Clearly, regions of low correlation magnitude (dark areas in Figure 4) are on the sides of the image and correspond to the regions where, during deformations, parts of the phantom extended beyond the imaged region and, therefore, can no longer be tracked.

Figure 4: A map of a normalized correlation coefficient displayed using a quantitative gray scale over 0.95-1.0 dynamic range. This image can be used to assess the quality of speckle tracking, i.e., how well the internal motion is measured.

The corresponding map of the vertical or axial displacement (Fig. 5a) reveals that there is no motion near the transducer (white areas), and motion towards the transducer is increasing with depth reaching maximum displacement near the bottom (dark areas). Here full black represents a 6 mm displacement toward the transducer, and full white corresponds to no displacement. Since acquired ultrasonic data are referenced relative to the transducer, it appears that the transducer is stationary and the bottom of the phantom moves toward it. The azimuthal displacement is presented in Fig. 5b where full black represents a 6 mm displacement to the left, full white represents a 6 mm displacement to the right, and mid-gray corresponds to no displacement. Due to diffraction limit of the transducer, the lateral displacements have smaller signal-to-noise ratio (SNR) compared to axial displacement estimates.

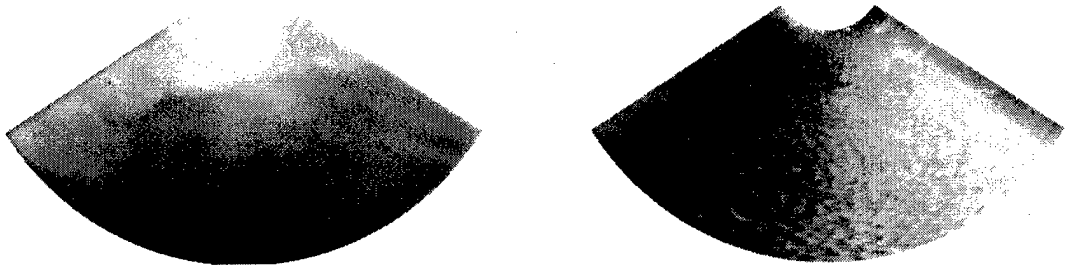

Figure 5: Axial (a) and azimuthal (b) displacement images of the prostate phantom.

The corresponding strain image is presented in Figure 6 where the distribution of normal axial strain (ε_{22}) is displayed using a quantitative color map, where full black corresponds to no strain and lower, and full white corresponds to –25% strain and higher.

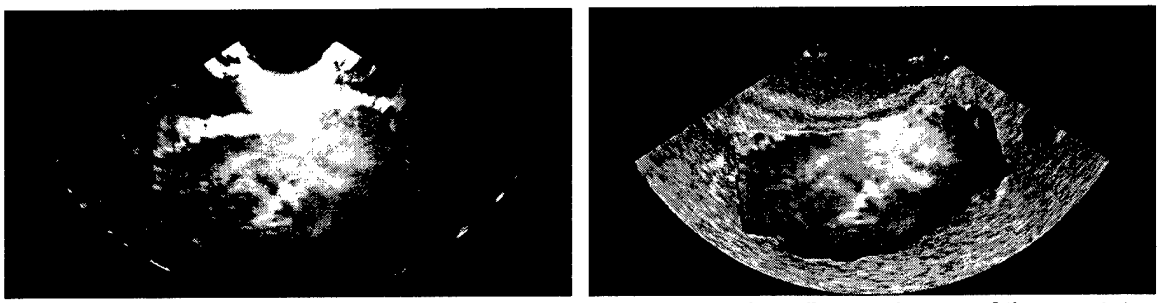

Figure 6: Strain image (a) and strain image overlaid on top of the B-scan image of the prostate before the injection of glutaraldehyde.

The strain is negative, indicating that sample size was reduced in the axial (vertical) direction. Larger strain magnitudes (yellow to white regions) signal softer material, and vice versa. From the strain image in Fig. 6, the fatty tissue surrounding the prostate is extremely soft, "absorbing" most of the deformation (high strain amplitude), and the overall prostate is significantly harder (low strain) compared to the fatty tissue. No elasticity contrast within prostate tissue is present, but this is expected for the normal prostate.

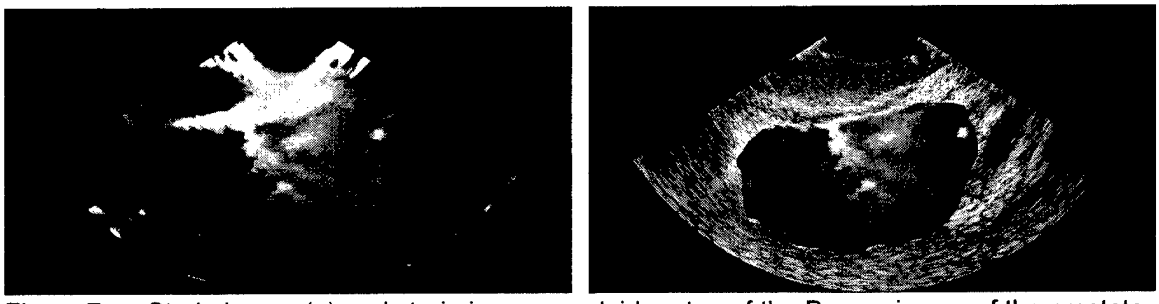

Figure 7: Strain image (a) and strain image overlaid on top of the B-scan image of the prostate after the injection of glutaraldehyde. Note the dark, low strain region on the left hand side of the prostate indicating harder tissue.

Finally, the strain images of the prostate after the injection of glutaraldehyde are presented in Figure 7. Note the darker area on the left hand side of the prostate. The localized reduction of the strain magnitude is in the region of injection and appears as an approximately circular dark region. This corresponds to the overall lower strain magnitude within the prostate after injection indicating an increase in tissue stiffness.

Manual palpation of the prostate cross-section also clearly indicated that this region was much harder than neighboring tissue.

The images presented in Figs. 6 and 7 suggests that for prostate elasticity imaging applications, the prostate carcinoma and other lesions can be easily detected given the adequate resolution of the imaging system.

KEY RESEARCH ACCOMPLISHMENTS:

- Design and build gel-based prostate mimicking phantoms to address mechanical and ultrasound properties of normal prostate and prostate abnormalities.
- Design and construct the deformation system capable of producing controlled deformation of the prostate phantoms. The ultrasound probe will be incorporated into the deformational system to closely resemble the clinically relevant environment of transrectal ultrasound (TRUS) examination of the prostate.
- Develop and/or modify existing algorithms for ultrasound speckle tracking, strain imaging and adaptive elasticity mapping needed for prostate elasticity imaging. The geometry of the probe, prostate and surrounding tissue, imaging plane and scan format, and nature of externally produced deformation patterns will be considered. In addition, controlled deformation and free-hand deformations will be considered.
- Test initially the performance of prostate elasticity imaging using tissue-mimicking phantoms.
- Conduct initial *ex-vivo* experiments to investigate the capabilities of prostate elasticity imaging including strain hardening.

REPORTABLE OUTCOMES:

S.R. Aglyamov, A.R. Skovoroda, J.M. Rubin, M. O'Donnell, and S.Y. Emelianov, "Model based reconstructive elasticity imaging of deep venous thrombosis," submitted for publication to the IEEE Transactions on Ultrasonics, Ferroelectrics, and Frequency Control (2003).

"Cancer Detection and Diagnosis using Combined Ultrasound, Optoacoustic and Elasticity Imaging" – Advanced Technology Program 2003, PI: Dr. S. Emelianov (submitted to Texas Higher Education Coordinating Board, August 2003)

Note: The results presented here represent the product of yet unfunded work. This is due to the fact that both Principal Investigator of this project, Dr. Emelianov, and Co-Investigator, Dr. Aglyamov, moved to the University of Texas at Austin during summer of 2002. The proposed work, however, did not stop although no expenses have occurred. Consequently, not all of the reportable outcomes are yet available while we are actively pursuing all necessary stages of the project.

CONCLUSIONS:

Elasticity imaging in the prostate is practical and feasible. First, since the elastic modulus in the prostate is expected to change by orders of magnitude with malignant lesions, and to a lesser extent with other types of lesions, it is anticipated that combined ultrasound, elasticity and strain-hardening imaging may detect and differentiate prostate pathology earlier than transrectal ultrasound (TRUS) examination alone or measurements of serum prostate-specific antigen (PSA) concentration. Second, based on current clinical criteria, transrectal ultrasound is already widely used for prostate diagnosis as well as laboratory measurements, and therefore, all necessary pre-requisites for elasticity imaging of the prostate are readily available. Patients will not be subjected to any additional biopsies, and the examination time will not increase to perform elasticity measurements of the prostate. Third, an urgent need exists for a more sensitive, specific, and earlier marker of prostate cancer - combined ultrasound, elasticity and strain-hardening imaging technique may fill that need and become an important clinical tool of sufficient sensitivity and specificity for early diagnosis and improved therapy of prostate cancer.

REFERENCES:

American Cancer Society. *Cancer Facts and Figures 2002.* Atlanta, Georgia: American Cancer Society; 2002.

Chenevert TL, Emelianov SY, and Skovoroda AR, "Elasticity Reconstructive Imaging Using Static Displacement and Strain Estimations," in 1997 Proceedings of the International Society of Magnetic Resonance in Medicine, p. 461, 1997

Chenevert TL, Skovoroda AR, O'Donnell M, and Emelianov SY, "Elasticity reconstructive imaging via stimulated echo MRI," Magnetic Resonance in Medicine, 39, pp. 482-490, 1998.

Emelianov SY, Lubinski MA, Weitzel WF, Wiggins RC, Skovoroda AR, and O'Donnell M, "Elasticity imaging for early detection of renal pathologies," Ultrasound in Medicine and Biology, 21(7):871-883, 1995a.

Emelianov SY, Skovoroda AR, Lubinski MA, and O'Donnell M, "Reconstructive Elasticity Imaging," in Acoustical imaging, 21, pp. 241-252 (Plenum press, New York, 1995b).

Emelianov SY, Swanson SD, Fowlkes JB, Rudenko OV, and Sarvazyan AP, "Remote Surrogate Palpation: Shear Wave Elasticity Imaging," Abstract of the 22nd Ultrasonic Imaging and Tissue Characterization Symposium, Ultrasonic Imaging, 19:61-62, 1997a.

Emelianov SY, Lubinski MA, Skovoroda AR, Erkamp RQ, Leavey SF, Wiggins RC, and O'Donnell M, "Reconstructive ultrasound elasticity imaging for renal pathology detection," Proceedings of the 1997 IEEE Ultrasonics Symposium, 1997b.

Emelianov SY, Erkamp RQ, Lubinski MA, Skovoroda AR, and O'Donnell M, "Non-linear tissue elasticity: Adaptive elasticity imaging for large deformations," Proceedings of the 1998 IEEE Ultrasonics Symposium, 2, pp. 1753-1756, 1998.

Emelianov SY, Lubinski MA, Skovoroda AR, Erkamp RQ, Leavey SF, Wiggins RC, and O'Donnell M, "Reconstructive ultrasound elasticity imaging for renal transplant diagnosis: kidney ex-vivo results," to appear in Ultrasonic Imaging, 2000.

Gao L, Parker KJ, Lerner RM, and Levinson SF, "Imaging of the elastic properties of tissue - a review," Ultrasound in Medicine and Biology, 22:959-977, 1996.

O'Donnell M, Emelianov SY, Skovoroda AR, Lubinski MA, Weitzel WF, and Wiggins RC, "Quantitative Elasticity Imaging," in 1993 IEEE Ultrasonic Symposium Proceedings 2:893-903, 1993.

O'Donnell M, Skovoroda AR, Shapo BM, and Emelianov SY, "Internal displacement and strain imaging using ultrasonic speckle tracking," IEEE Transactions on Ultrasonics, Ferroelectrics, and Frequency Control, 41:314-325, 1994.

Ophir J, Cespedes I, Garra B, Ponnekanti H, Huang Y, Maklad N, "Elastography: ultrasonic imaging of tissue strain and elastic modulus in vivo," European Journal of Ultrasound, 3:49-70, 1996.

Sarvazyan AP, "Low frequency acoustic characteristics of biological tissues," Mechanics of Polymers, 4:691-695, 1975.

Sarvazyan A, Maevsky E, Gukasian D, Skovoroda A, Emelianov S, Berzhanskaja Y, Oranskaja G and Klishko A, "On the diagnostic value of ultrasound elasticity imaging of the breast", abstract of the 1993 IEEE Ultrasonics Symposium (1993).

Sarvazyan AP, Skovoroda AR, Emelianov SY, Fowlkes JB, Pipe JG, Adler RS, Buxton RB, and Carson PL, "Biophysical bases of elasticity imaging," In: Acoustical Imaging 21, J.P. Jones (ed), Plenum Press, New York, pp. 223-240 (1995).

Silverberg E, Lubera JA, "Cancer Statistics," CA Cancer J Clin., 39(1):3-20, 1989

Skovoroda AR, Emelianov SY, Lubinski MA, Sarvazyan AP, and O'Donnell M, "Theoretical analysis and verification of ultrasound displacement and strain imaging," IEEE Transactions on Ultrasonics, Ferroelectrics, and Frequency Control, 41:302-313, 1994.

Skovoroda AR, Emelianov SY, and O'Donnell M, "Reconstruction of tissue elasticity based on ultrasound displacement and strain images," IEEE Transactions on Ultrasonics, Ferroelectrics, and Frequency Control, 42:747-765, 1995.

Skovoroda AR, Lubinski MA, Emelianov SY, and O'Donnell M, "Nonlinear estimation of the lateral displacement using tissue incompressibility," IEEE Transactions on Ultrasonics, Ferroelectrics, and Frequency Control, 45, pp. 491-503, 1998.

Skovoroda AR, Lubinski MA, Emelianov SY, and O'Donnell M, "Reconstructive elasticity imaging for large deformations," IEEE Transactions on Ultrasonics, Ferroelectrics, and Frequency Control, 46, pp. 523-535, 1999.

APPENDICES:

None